0090-9556/07/3510-1766–1780$20.00
DRUG METABOLISM AND DISPOSITION
Vol. 35, No. 10
15644/3252832
DMD 35:1766–1780, 2007
Printed in U.S.A.
Copyright © 2007 by The American Society for Pharmacology and Experimental Therapeutics

Prediction of Human Pharmacokinetics Using Physiologically Based Modeling: A Retrospective Analysis of 26 Clinically Tested Drugs

Stefan S. De Buck, Vikash K. Sinha, Luca A. Fenu, Marjoleen J. Nijsen, Claire E. Mackie, and Ron A. H. J. Gilissen

Johnson & Johnson Pharmaceutical Research and Development, Discovery ADME-Tox Department, Beerse, Belgium

Received March 5, 2007; accepted July 3, 2007

ABSTRACT:

The aim of this study was to evaluate different physiologically based modeling strategies for the prediction of human pharmacokinetics. Plasma profiles after intravenous and oral dosing were simulated for 26 clinically tested drugs. Two mechanism-based predictions of human tissue-to-plasma partitioning (P_{tp}) from physicochemical input (method Vd1) were evaluated for their ability to describe human volume of distribution at steady state (V_{ss}). This method was compared with a strategy that combined predicted and experimentally determined in vivo rat P_{tp} data (method Vd2). Best V_{ss} predictions were obtained using method Vd2, providing that rat P_{tp} input was corrected for interspecies differences in plasma protein binding (84% within 2-fold). V_{ss} predictions from physicochemical input alone were poor (32% within 2-fold). Total body clearance (CL) was predicted as the sum of scaled rat renal clearance and hepatic clearance projected from in vitro metabolism data. Best CL predictions were obtained by disregarding both blood and microsomal or hepatocyte binding (method CL2, 74% within 2-fold), whereas strong bias was seen using both blood and microsomal or hepatocyte binding (method CL1, 53% within 2-fold). The physiologically based pharmacokinetics (PBPK) model, which combined methods Vd2 and CL2 yielded the most accurate predictions of in vivo terminal half-life (69% within 2-fold). The Gastroplus advanced compartmental absorption and transit model was used to construct an absorption-disposition model and provided accurate predictions of area under the plasma concentration-time profile, oral apparent volume of distribution, and maximum plasma concentration after oral dosing, with 74%, 70%, and 65% within 2-fold, respectively. This evaluation demonstrates that PBPK models can lead to reasonable predictions of human pharmacokinetics.

In the drug discovery process considerable resources are required to assess the pharmacokinetic (PK) properties of potential drug candidates in vivo in animals. To optimize the use of such in vivo testing, there has been a growing interest in predicting the PK behavior of drug candidates (Theil et al., 2003; van de Waterbeemd and Gifford, 2003). If sufficiently reliable, such simulations could also help to select the most promising candidates for development and reject those with a low probability of success (van de Waterbeemd and Gifford, 2003).

The majority of the approaches to predict human PK developed to date typically focus on the drug's behavior in individual processes of absorption, distribution, metabolism and excretion (ADME). The characterization of a drug's PK in a complex biological system is best described by assembling these processes in one global model. In this context, physiologically based pharmacokinetics (PBPK) models have been developed (Bischoff, 1986). PBPK models map the complex drug transport scheme onto a physiologically realistic compartmental structure (Fig. 1). The major structural elements of the PBPK disposition model are derived from the anatomical structure of the organism; therefore, the model structure is predetermined and basically independent of the drug of interest. The PBPK model input parameters include both a drug-independent and a drug-specific subset. The first subset comprises data underlying the physiological processes (e.g., blood flow), and the second subset comprises drug-specific biochem-

Article, publication date, and citation information can be found at http://dmd.aspetjournals.org.
doi:10.1124/dmd.107.015644.

ABBREVIATIONS: PK, pharmacokinetic(s); ACAT, advanced compartmental absorption and transit model; ADME, absorption, distribution, metabolism, and excretion; AUC, area under the plasma concentration-time curve; AUMC, area under the first moment curve; BCS, Biopharmaceutical Classification Scheme; CL, total body clearance from plasma; CL/*F*, total body clearance from plasma after oral administration; CL_H, hepatic plasma clearance; $CL_{H,blood}$, hepatic blood clearance; CL_{int}, intrinsic clearance; CL_R, renal clearance from plasma; C_{max}, peak plasma concentration after oral administration; *D*, dose; *F*, absolute oral bioavailability; fu_{inc}, unbound fraction in microsomal or hepatocyte incubation; fu_p, unbound fraction in plasma; GFR, glomerular filtration rate; in vivo $t_{1/2}$, in vivo terminal half-life; log P_{ow}, *n*-octanol:water partition coefficient of the non-ionized species; PBPK, physiologically based pharmacokinetics; P_{tp}, tissue-to-plasma partition coefficient; P_{tpu}, tissue-to-plasma partition coefficient of the unbound drug; Q_h, hepatic blood flow; RA, ratio of albumin concentration found in tissue over plasma; R_B, blood-to-plasma concentration ratio; SF, scaling factor; SIF, simulated intestinal fluid; V_d/F, apparent volume of distribution after oral administration; V_{ss}, apparent volume of distribution at steady state.

DOCKET ALARM
Find authenticated court documents without watermarks at docketalarm.com.

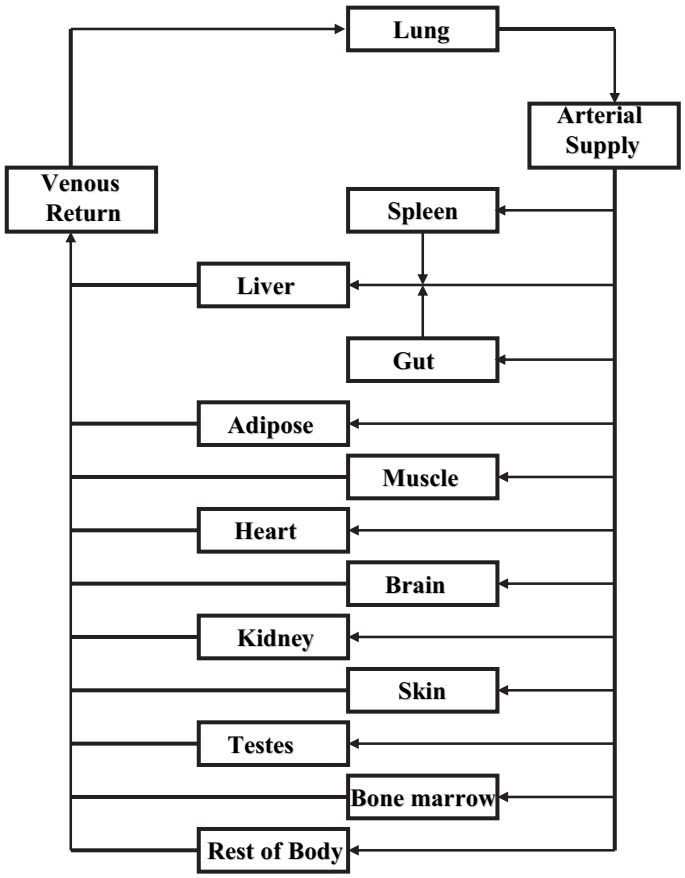

FIG. 1. Scheme of the generic disposition PBPK model for simulation of full plasma and tissue concentration-time profiles in rat and human. An overview of all physiological values is given in Table 3. Estimation of rate and extent of oral absorption from the gut was obtained using ACAT (Yu and Amidon, 1999; Agoram et al., 2001). For more details on all methods used, refer to *Materials and Methods*.

ical parameters. The latter consists of the drug's in vivo intrinsic clearance (CL_{int}) of each organ involved in its elimination, in addition to estimates of the drug's tissue-to-plasma coefficient (P_{tp}) for each model compartment. Prediction of the rate and extent of absorption can be obtained using semiphysiologically based absorption models, such as the advanced compartmental absorption and transit (ACAT) model (Yu and Amidon, 1999; Agoram et al., 2001). As depicted in Fig. 1, the ACAT model may serve as a time-dependent input function to the disposition model, thereby creating a combined absorption-distribution PBPK model.

Although PBPK models have been widely used in areas such as risk assessment to predict the PK behavior of toxic chemicals, their application in support of drug discovery and development has remained limited, most probably as a result of their mathematical complexity and the labor-intensive drug-specific input data required. However, more recently, a variety of in vitro based prediction tools have been developed for the estimation of PBPK model input parameters (Theil et al., 2003). Such prediction tools require commonly determined biochemical and physicochemical drug-specific input and thus allow for the prediction of ADME parameters before any in vivo experiment. As examples of such prediction tools, mechanistic equations have been developed for the prediction of fraction of oral dose absorbed (Agoram et al., 2001; Willmann et al., 2004), tissue partitioning (P_{tp}) (Poulin and Theil, 2000; Poulin et al., 2001; Rodgers et al., 2005a), apparent volume of distribution at steady state (V_{ss}) (Poulin and Theil, 2002), and hepatic plasma clearance (CL_H) (Houston, 1994; Obach et al., 1997; Rodgers et al., 2005b). In a previous study, we also evaluated a variety of physiologically based prediction tools for the prediction of rat PK (De Buck et al., 2007).

The aim of the present work was to further evaluate these prediction tools for their ability to predict human PK parameters by simulation of full plasma concentration-time profiles after both intravenous and oral administration. Although recent studies have addressed a similar question, the overall prediction accuracy obtained was in the lower range, particularly for predictions of V_{ss} and in vivo terminal half-life (in vivo $t_{1/2}$) (Parrott et al., 2005b; Jones et al., 2006a). In the present study, a more comprehensive range of approaches toward the prediction of V_{ss} and CL_H was explored, including two mechanism-based V_{ss} predictions from physicochemical input, as well as approaches that combine the use of both predicted and experimentally determined in vivo rat P_{tp}. For each of the approaches tested, the influence of interspecies differences in plasma protein binding on prediction accuracy was investigated. The role of relative drug binding in plasma and in vitro drug matrices was also considered with respect to CL_H projection from in vitro metabolism data. Whereas the basic tenet of pharmacokinetics states that the unbound drug concentration in the plasma dictates clearance, our previous report in rat using microsomes has suggested that in vitro CL_{int} may provide a better estimate of in vivo CL_H of total rather than unbound drug (De Buck et al., 2007). To further investigate the effect of relative drug binding, predictions of human CL_H were performed each time under two variations, either by incorporating or disregarding such binding factors. Methods to predict V_{ss} and CL were combined to predict in vivo $t_{1/2}$, and the ACAT model was tested for its ability to predict the area under the oral concentration-time profile (AUC), the oral apparent volume of distribution (V_d/F), and peak plasma concentration (C_{max}). To determine whether a successful prediction in rat correlates with a successful prediction in human, the accuracy of each method was assessed within both species.

Materials and Methods

Compounds and Sources of in Vitro and in Vivo Parameters. The set of compounds ($n = 26$) included in this analysis were taken from those brought into clinical development at Johnson & Johnson Pharmaceutical Research and Development (Beerse, Belgium). Compounds were selected based on the availability of historical data on the in vivo preclinical (rat) and clinical PK, as well as of each of the following experimentally determined biochemical and physicochemical parameters: unbound fraction in plasma (fu_p), unbound fraction in microsomal or hepatocyte incubation (fu_{inc}), basic and acidic dissociation constants (pK_a), *n*-octanol:water partition coefficient of the non-ionized species ($\log P_{ow}$), aqueous solubility at defined pH conditions or solubility in simulated intestinal fluid (SIF), in vitro CL_{int} determined in hepatic microsomes or hepatocyte suspension cultures, and the blood-to-plasma concentration ratio (R_B). Summaries of the available in vitro and in vivo PK data are shown in Tables 1 and 2, respectively.

The 26 compounds in the data set cover a broad range of small molecules from a variety of discovery programs. The majority of compounds ($n = 19$) were moderate-to-strong bases (pK_a of protonated base >7.0); three were neutral or weakly ionized at physiological pH (weak base). The remaining compounds were one weak acid, one strong acid, and two zwitterions. The lipophilicity ($\log P_{ow}$) ranged between 1.11 and 5.5, and fu_p ranged from 0.001 to 0.867. Aqueous solubility was highly variable with values at physiological pH ranging from 0.003 mg/ml to 74 mg/ml. V_{ss} in humans varied from limited (30 L) to widespread (>1000 L). In the rat, major elimination pathways included hepatic metabolism, renal excretion, or a combination of the two. In humans, total body clearance from plasma (CL) varied from less than 10% of hepatic blood flow (Q_h) to more than 70% of Q_h.

Model Structure. The Gastroplus 5.1.0 generic PBPK model and its built-in mass balance differential equations were used for all simulations (Simulations Plus Inc., Lancaster, CA). In brief, the model (Fig. 1) was composed of 14 tissue compartments, including lung, spleen, liver, gut, adi-

DOCKET ALARM Find authenticated court documents without watermarks at docketalarm.com.

TABLE 1

In vitro and in silico physicochemical and biochemical properties of the 26 compounds

JNJ No.	Generic Name	mol. wt.	pK_a	Log P_{ow}	Species	fu_p	fu_{inc}[a]	R_B	In Vivo CL_{int}[b]	Test System	P_{eff}[c,d]	Solubility
									ml/min/kg		*10^{-4} cm/s*	*mg/ml*
JNJ1	Lorcainide	407	B 9.44	4.16	Rat	0.260		1.2	624	RLMic	4.78	265, 214, 192, 2.4, 0.18 in aqueous buffer at pH 2.2, 4.2, 5.9, 7.7 and 9.5, respectively
					Human	0.150	0.45	0.70	31.5	HLMic		
JNJ2	Domperidone	425	B 7.89 B 2.50	3.96	Rat	0.092		1.3	178	RLMic	1.88	0.31, 1.5, 0.057, 0.006, 0.001 in aqueous buffer at pH 2.3, 4.2, 6.0, 7.2, and 8.0, respectively
					Human	0.061	0.34	0.74	69.3	HLMic		
JNJ3	Nebivolol	405	B 8.40	4.03	Rat	0.015		1.2	89.1	RLMic	1.86	0.046, 0.071, 0.91, 0.031, 0.12 in aqueous buffer at pH 1.9, 4.0, 5.4, 6.1, and 8.1, respectively
					Human	0.020	0.12[e]	1.2	11.2	HLMic		
JNJ4	Galantamine	287	B 8.20	1.11	Rat	0.755		1.0	20.8	RLMic	5.43	35, 39, 33, 38, 37, 41 in aqueous buffer at pH 2.0, 4.9, 5.2, 6.8, 7.5, and 7.7, respectively
					Human	0.822	0.86[e]	1.2	2.49	HLMic		
JNJ5	Alfentanil	416	B 6.50	2.21	Rat	0.164		0.69	416	RLMic		
					Human	0.079	0.97	0.63	190	HLMic		
JNJ6	Sufentanil	386	B 8.10	4.02	Rat	0.069		0.74	250	RLMic		
					Human	0.075	0.87	0.74	184	HLMic		
JNJ7	Ketanserin	395	B 7.50	3.30	Rat	0.012		0.65	10.0	RLMic	7.14	0.72, 1.30, 16, 15, 11, 0.050, 0.001 in aqueous buffer at pH 1.2, 2.6, 3.1, 3.5, 4.6, 5.7, and 8.0, respectively
					Human	0.049	0.32	0.70	31.5	HLMic		
JNJ8	Ritanserin	478	B 8.20 B 2.07	5.20	Rat	0.015		0.74	139	RLMic	12.0[d]	1.4, 0.063, 0.037in aqueous buffer at pH 2.2, 4.1, and 6.1, respectively
					Human	0.008	0.45	0.65	4.91	HLMic		
JNJ9	Sabeluzole	415	B 7.60 B 3.40	4.63	Rat	0.016		0.84	43.0	RLMic	2.93	13, 5.8, 1.3, 3.9, 0.19, 0.01 in aqueous buffer at pH 2.7, 3.3, 4.2, 4.6, 6.0, and 6.9, respectively
					Human	0.014	0.06	0.82	5.10	HLMic		
JNJ10		297	B 9.47	4.03	Rat	0.141		2.0	312	RLMic	0.321	29, 11, 4.7, 2.9, 0.14, 0.061 in aqueous buffer at pH 3.4, 3.5, 4.5, 7.5, 9.14, and 12.8, respectively
					Human	0.115	0.12[e]	1.4	10.5	HLMic		
JNJ11	Lubeluzole	433	B 7.60 B 4.27	4.88	Rat	0.008		0.76	52.0	RLMic	2.79	0.013 in aqueous buffer at pH 6.9
					Human	0.003	0.05[e]	0.58	3.90	HLMic		
JNJ12		296	B 9.88 B 3.00	1.18	Rat	0.820		1.5	20.8	RLMic	0.05	20, 20, 20, 7.56, 3.09 in aqueous buffer at pH 1.8, 3.8, 4.3, 7.45, and 12.6, respectively
					Human	0.867	0.85[e]	1.5	0.570	HLMic		
JNJ13	Ridogrel	366	A 4.90 B 3.84	3.54	Rat	0.049		0.80	5.10	RLHep	4.73	0.26, 0.02, 0.65, 9.8 in aqueous buffer at pH 2.1, 5.4, 7.0, and 8.1, respectively
					Human	0.033	1.0[f]	0.77	2.20	HLHep		
JNJ14	Laniquidar	584	B 7.90 B 3.30	5.50	Rat	0.002		0.79	51.7	RLMic	4.56[d]	12.4, 0.58, 0.10, 0.064 in aqueous buffer at pH 2.21, 2.78, 3.62, and 7.05, respectively
					Human	0.001	0.08	0.62	99.0	HLMic		
JNJ15	Mazapertine	421	B 7.06	3.96	Rat	0.030		0.63	623	RLMic	5.70[d]	80, 43, 0.54, 0.21, 0.22 in aqueous buffer at pH 3.8, 4.7, 6.9, 8.9, and 11.5, respectively
					Human	0.011	0.13[e]	0.52	231	HLMic		
JNJ16		686	B 7.20 B 3.10	4.12	Rat	0.036		0.78	28.2	RLMic	1.85	13, 1.1, 0.75, 0.04, 0.01 in aqueous buffer at pH 2.2, 3.7, 5.7, 7.5, and 8.6, respectively
					Human	0.034	0.08	0.75	20.3	HLMic		
JNJ17		558	B 7.26 B 6.18 B 4.00 A 8.28	3.90	Rat	0.028		1.0	416	RLMic		
					Human	0.009	0.14[e]	1.0	231	HLMic		
JNJ18	Risperidone	411	B 8.24 B 3.11	3.04	Rat	0.118		0.85	250	RLMic	5.70	40, 4.1, 1.8, 0.25, 0.064 in aqueous buffer at pH 5.4, 6.0, 6.2, 7.5, and 8.7, respectively
					Human	0.100	0.34	0.67	7.96	HLMic		
JNJ19	Levocabastine	420	B 9.90 A 3.20	1.75	Rat	0.465		1.1	1.25	RLHep	2.10	0.06, 0.05, 0.02, 0.02 in aqueous buffer at pH 2.0, 3.2, 6.0, and 8.0, respectively
					Human	0.453	1.0[f]	1.2	0.33	HLHep		
JNJ20	Norcisapride	313	B 9.10 B 3.00	1.51	Rat	0.650		1.5	2.43	RLMic	1.16	80, 92, 93, 74, 41 in aqueous buffer at pH 2.1, 4.8, 6.6, 7.8, and 8.0, respectively
					Human	0.625	0.79[e]	1.6	0.88	HLMic		

DOCKET ALARM
Find authenticated court documents without watermarks at docketalarm.com.
Apotex v. Cellgene - IPR2023-00512
Petitioner Apotex Exhibit 1039-0003

TABLE I—*Continued*

NJ No.	Generic Name	mol. wt.	pK_a	Log P_{ow}	Species	fu_p	fu_{inc} [a]	R_B	In Vivo CL_{int} [b]	Test System	P_{eff} [c,d]	Solubility
									ml/min/kg		10^{-4} *cm/s*	*mg/ml*
NJ21		481	B 7.27	3.55	Rat	0.015		1.5	35.6	RLMic	1.96	0.05 in aqueous buffer at pH 1.2, 0.003 in SIF at pH 7.53
					Human	0.012	0.23	1.5	77.0	HLMic		
NJ22		570	A 8.21	4.78	Rat	0.001		0.74	156	RLMic	0.751	0.002 and 100 in aqueous buffer at pH 6.5 and 8.7, respectively and 0.249 in SIF at pH 7.5
					Human	0.001	0.90	0.55	116	HLMic		
NJ23		359	B 7.00 B 3.10	3.40	Rat	0.082		0.80	208	RLMic	3.41	10.3, 3.9, 0.42, 0.035, 0.002 in aqueous buffer at pH 3.0, 4.2, 5.1, 6.0, and 8.1, respectively
					Human	0.016	0.06	0.61	10.2	HLMic		
NJ24		380	B 7.23 B 5.20	5.24	Rat	0.007		0.75	371	RLHep	2.00	20, 10.2, 2.19, 0.026 in aqueous buffer at pH 1.4, 4.4, 5.2, and 6.0, respectively and 0.005 SIF at pH 7.4
					Human	0.006	1.0[f]	0.59	8.97	HLHep		
NJ25		660	B 6.80 B 2.86	4.84	Rat	0.015		0.70	19.9	RLMic	4.54[d]	1.6, 2.43, 0.52, 0.02, 0.01 in aqueous buffer at pH 2.1, 4.4, 5.0, 7.0, and 9.0, respectively
					Human	0.016	0.05[e]	0.72	7.28	HLMic		
NJ26		500	B 5.95 B 3.67	4.00	Rat	0.036		1.3	24.8	RLHep	2.07	2.3, 0.18, 0.014, 0.005 in aqueous buffer at pH 2.3, 4.5, 5.9, and 7.5
					Human	0.023	1.0[f]	1.5	9.03	HLHep		

A, acid; B, base; HLHep, human liver hepatocytes; HLMic, human liver microsomes; log RLHep, rat liver hepatocytes; RLMic, rat liver microsomes.
[a] Experimental values of fu_{inc} in human microsomal protein were determined according to the method of Giuliano et al. (2005). Rat fu_{inc} was assumed to equal human fu_{inc}.
[b] In vivo CL_{int} was calculated using eq. 6 as described under *Materials and Methods*.
[c] Permeability was measured using a Caco-2 assay and converted to P_{eff} using the reported correlation log $P_{eff,human} = 0.6532 \cdot \log P_{app,caco-2} - 0.3036$ (Sun et al., 2002).
[d] In silico predicted P_{eff} (ADMETPredictor software version 1.30.2; Simulations Plus Inc.).
[e] Predicted fu_{inc} value in microsomes was determined according to the method of Austin et al. (2002).
[f] Hepatocyte incubation was performed in protein-free medium ($fu_{inc} = 1$).

marrow, and rest of the body, which were linked by the venous and arterial blood circulation. It was assumed that drug distributes instantaneously and homogenously within each tissue compartment, and uptake of drug within each tissue compartment was limited by the blood flow (perfusion rate-limited uptake). The default Gastroplus settings of all physiological data used in the rat and human PBPK models are summarized in Table 3. The methods used for estimating the PBPK model input data on CL_H, renal plasma clearance (CL_R), P_{tp} values, and absorption rate are described below.

Prediction of Human and Rat P_{tp} and V_{ss}: Method Vd1. Predicted values of rat and human P_{tp} for each tissue compartment of Fig. 1 were obtained from drug-specific physicochemical parameters using the following mechanistic tissue composition-based equation developed by Poulin and coworkers (Poulin and Theil, 2002):

$$P_{tp} = \frac{[P \cdot (V_{NLT} + 0.3 \cdot V_{PHT}) + (V_{WT} + 0.7 \cdot V_{PHT})] \cdot fu_p}{[P \cdot (V_{NLp} + 0.3 \cdot V_{PHp}) + (V_{Wp} + 0.7 \cdot V_{PHp})] \cdot fu_t} \quad (1)$$

where P is the anti-logged value of log P_{ow} for a nonadipose tissue or is the vegetable oil/buffer partition coefficient for both the ionized and nonionized species at pH 7.4 (D_{vow}) for adipose tissue. D_{vow} was calculated from log P_{ow} using the Henderson-Hasselbalch equations and the following relationship: log $P_{vow} = 1.115 \cdot \log P_{ow} - 1.35$ (Leo et al., 1971). V is the fractional tissue volume content of neutral lipids (NL), phospholipids (PH), or water (W) in tissue (T) and plasma (p). The physiological data on human and rat values used for V_{NLT}, V_{NLp}, V_{PHT}, V_{PHp}, V_{WT}, and V_{Wp} have been described in the literature (Poulin and Theil, 2002). The fraction unbound in tissue (fu_t) in eq. 1 was estimated as follows:

$$fu_t = 1/(1 + (((1 - fu_p)/fu_p) \cdot RA)) \quad (2)$$

where RA is the ratio of albumin concentration found in tissue over plasma. For lipophilic and highly protein-bound compounds, it has been assumed that for adipose tissue, RA equals 0.15, whereas for nonadipose tissue, RA equal 0.5 (Ellmerer et al., 2000; Poulin and Theil, 2002).

Finally, rat and human V_{ss} values were calculated by Gastroplus software according to the equation of Sawada et al. (1984) in which V_{ss} equals the plasma volume in addition to the sum of each P_{tp} multiplied by its respective tissue volume.

Prediction of Human and Rat P_{tp} and V_{ss}: Method Vd2. For rat P_{tp} and V_{ss}, experimental rat P_{tp} values were determined under in vivo conditions (single oral or intravenous dose) as the ratio of the AUC calculated over a minimum of five time points, assuming pseudoequilibrium. All experimentally determined in vivo rat P_{tp} values used within this study are summarized in Table 2. In instances where the in vivo P_{tp} was not available for a compound, the value for that tissue compartment (Fig. 1) was predicted using the tissue composition-based equation as described by Rodgers et al. (2005a). In brief, for strong bases ($pK_a > 7.0$), P_{tp} of unbound drug (P_{tpu}) was calculated using eq. 3:

$$P_{tpu} = \frac{P_{tp}}{fu_p} = \left[V_{EW} + \frac{1 + 10^{pKa-7.0}}{1 + 10^{pKa-7.4}} \cdot V_{IW} + \frac{K_a \cdot [AP]_t \cdot 10^{pKa-7.0}}{1 + 10^{pKa-7.4}} + \frac{P_{vow} \cdot V_{NL} + ((0.3 \cdot P_{vow} + 0.7) \cdot V_{NP})}{1 + 10^{pKa-7.4}} \right] \quad (3)$$

where V is the fractional tissue volume of neutral lipids (NL), neutral phospholipids (NP), extracellular water (EW), and intracellular water (IW), $[AP]_t$ is the concentration of acidic phospholipids in tissue, all physiological data on V_{EW}, V_{IW}, V_{NL}, V_{NP} and $[AP]_t$ for both adipose and nonadipose tissue have been described in the literature (Rodgers et al., 2005a), pK_a represents the dissociation constant of the protonated base, and P_{vow} is the anti-logged value of log P_{vow} (calculated from P_{ow} as described above). K_a is the association constant of the compound with the acidic phospholipids, and was calculated

DOCKET ALARM Find authenticated court documents without watermarks at docketalarm.com.

TABLE 2

Summary of the preclinical (rat) and clinical pharmacokinetic data for the 26 compounds

NJ No.	Species	Dose	Route	CL or CL/*F*	CL_R	V_{ss} or V_d/F	In Vivo $t_{1/2}$	C_{max}	AUC	Experimentally Determined In Vivo Rat P_{tp}[a]										
										Lung	Adipose	Muscle	Liver	Spleen	Heart	Brain	Kidney	Skin	Testes	Bone
		mg		*l/h*		*liters*	*h*	*ng/ml*	*ng · h/ml*											
NJ1	Human	100	i.v.	71.6		413	5.10		1.40E + 03											
	Human	100	p.o.	202		1.49E + 03		60.1	494											
	Rat	2.50	i.v.	1.55		3.92	2.91		1.61E + 03	19.4	5.27	6.50	0.571	10.3	2.91	1.52	5.68			
	Rat	1.88	p.o.	4.24					442											
NJ2	Human	10.0	i.v.	34.3		157	7.59		292											
	Human	60.0	p.o.	232		2.54E + 03		102	259											
	Rat	0.625	i.v.	1.30		1.39	0.871		480	10.9	3.21	3.45	13.8		3.87		22.5	4.35		
	Rat	0.625	p.o.	6.01					104											
NJ3	Human	0.500	i.v.	80.5		1.14E + 03	10.40		6.20											
	Human	5.00	p.o.	192		2.87E + 03		2.01	26.1											
	Rat	0.313	i.v.	0.736		1.55	1.37		425	99.7	2.67	2.95	14.1	15.6	4.71	3.73	10.6	7.65	5.32	7.87;14.1
	Rat	0.313	p.o.	0.925					338											
NJ4	Human	8.00	i.v.	17.8	3.93	175	7.40		482											
	Human	8.00	p.o.	18.7		200		42.6	427											
	Rat	0.625	i.v.	0.473	0.100	1.30	3.48		1.32E + 03	4.42	0.476	2.14	2.53	2.92	2.28	1.51	14.5	1.14	1.46	4.79;4.81
	Rat	0.625	p.o.	0.803					778											
NJ5	Human	8.75	i.v.	21.2		28.8	1.37		510											
	Human		p.o.																	
	Rat	4.00E02	i.v.	0.464		0.110	0.146		86.2	1.11	3.01	0.440	1.43	1.05	0.791	0.181	1.18	0.512	0.481	
	Rat		p.o.																	
NJ6	Human	0.350	i.v.	49.6		128	2.47		8.10											
	Human		p.o.																	
	Rat	6.25E04	i.v.	1.04		0.967	1.05		0.604	6.18	7.72	1.71	0.370	2.80	1.80	2.08	1.17		1.97	
	Rat		p.o.																	
NJ7	Human	10.0	i.v.	33.9		268	14.3		298											
	Human	20.0	p.o.	71.7		1.48E + 03		71.4	279											
	Rat	2.50	i.v.	5.75E-02		0.168	2.00		4.35E + 04	1.49	0.562	0.284	2.60	0.911	0.354	0.194	1.53	0.463	0.495	0.19;0.18
	Rat	2.50	p.o.	9.82E02					2.55E + 04											
NJ8	Human	5.00	i.v.	2.14		99.0	40.0		2.51E + 03											
	Human	10.0	p.o.	2.33		134		164	4.30E + 03											
	Rat	0.625	i.v.	0.400		2.00	2.52		1.56E + 03	27.8	4.29	3.02	21.8			10.5	14.1			
	Rat	0.625	p.o.	0.918					681											
NJ9	Human	10.0	i.v.	17.0		385	18.9		594											
	Human	5.00	p.o.	22.7		621		14.5	220											
	Rat	0.313	i.v.	0.538		1.46	2.13		581	29.2	8.41	0.831	37.7	5.48	2.45	5.37	10.4	2.95	4.62	1.83;7.76
	Rat	0.625	p.o.	1.24					506											
NJ10	Human	1.00	i.v.	149		1.33E + 03	7.09		6.58											
	Human	8.00	p.o.	950		9.72E + 03		0.590	8.42											
	Rat	2.50	i.v.	2.02		8.37	2.77		1.24E + 03	400		20.1	150		40.2	80.3	80.1		75.1	
	Rat	10.0	p.o.	5.26					1.90E + 03											

DOCKET ALARM
Find authenticated court documents without watermarks at docketalarm.com.

Apotex v. Cellgene - IPR2023-00512
Petitioner Apotex Exhibit 1039-0005

DOCKET ALARM

Explore Litigation Insights

Docket Alarm provides insights to develop a more informed litigation strategy and the peace of mind of knowing you're on top of things.

Real-Time Litigation Alerts

Keep your litigation team up-to-date with **real-time alerts** and advanced team management tools built for the enterprise, all while greatly reducing PACER spend.

Our comprehensive service means we can handle Federal, State, and Administrative courts across the country.

Advanced Docket Research

With over 230 million records, Docket Alarm's cloud-native docket research platform finds what other services can't. Coverage includes Federal, State, plus PTAB, TTAB, ITC and NLRB decisions, all in one place.

Identify arguments that have been successful in the past with full text, pinpoint searching. Link to case law cited within any court document via Fastcase.

Analytics At Your Fingertips

Learn what happened the last time a particular judge, opposing counsel or company faced cases similar to yours.

Advanced out-of-the-box PTAB and TTAB analytics are always at your fingertips.

API

Docket Alarm offers a powerful API (application programming interface) to developers that want to integrate case filings into their apps.

LAW FIRMS
Build custom dashboards for your attorneys and clients with live data direct from the court.

Automate many repetitive legal tasks like conflict checks, document management, and marketing.

FINANCIAL INSTITUTIONS
Litigation and bankruptcy checks for companies and debtors.

E-DISCOVERY AND LEGAL VENDORS
Sync your system to PACER to automate legal marketing.